Variations in atmospheric composition over Northern Eurasia regions under weather and climate anomalies associated with atmospheric blocking events

Variations in atmospheric composition over Northern Eurasia regions under weather and climate anomalies associated with atmospheric blocking events

S A Sitnov[1] **and I I Mokhov**[1, 2]

[1] Obukhov Institute of Atmospheric Physics, Russian Academy of Sciences, Moscow, Russia
[2] Lomonosov Moscow State University, Moscow, Russia

sitnov@ifaran.ru

Abstract. Changes in the composition of the atmosphere associated with the atmospheric blocking events were analyzed using the measurements of ozone, water vapor, methane, formaldehyde, carbon monoxide, nitrogen dioxide, as well as aerosol optical characteristics from the satellite instruments OMI, MLS, AIRS, MODIS and MOPITT as well as ground-based, balloon and NCEP/NCAR reanalysis data. The changes in atmospheric composition associated with pyrogenic, biogenic and soil emissions of aerosol and gas constituents as well as the changes due to the regional peculiarities of the large-scale atmospheric dynamics are discussed.

1. Introduction

The continued global climate change increases the likelihood of regional weather and climate anomalies essentially affecting gas constituents and aerosol composition of the regional atmosphere. Extreme weather and climate events are associated with the prolonged impeding of the western air mass transfer in the mid-latitude troposphere, which is known as a phenomenon of atmospheric blocking [1]. Summer blocks are accompanied by heat wave, lack of rainfall and drought of soil, which promote the development of massive forest fires accompanied by pyrogenic emissions of various products of biomass combustion into the atmosphere [2]. Along with this, anomalous temperature rise as well as sunny and dry weather cause abiotic stress of vegetation in the blocking area [3] that as a protective reaction leads to the increased emissions of volatile organic compounds into the atmosphere by plants [4]. In permafrost regions, an increase in the land surface temperature (along with changes in soil moisture and water table) regulates the soil emission of carbonaceous compounds [5]. Along with changes associated with the pyrogenic, biogenic and soil emissions, the regional peculiarities of the large-scale atmospheric circulation associated with atmospheric blocks are responsible for changes in the composition of regional atmosphere [6-9].

The aim of this work is a multi-instrumental analysis of changes in the gas and aerosol composition of the atmosphere in the regions of Northern Eurasia under summer atmospheric blocking events. The relevance of this study is related to the fact that, according to model calculations, due to continued global warming, one can expect an increase in anomalously prolonged atmospheric blocking events [10].

2. Data used

The basis for the analysis was satellite data, namely the measurements of UV radiation, total column ozone (O_3), total column formaldehyde (CH_2O) and tropospheric column of nitrogen dioxide (NO_2) from the Ozone Monitoring Instrument (OMI) [11], the measurements of the vertical profiles of ozone from the Microwave Limb Sounder (MLS) [12], the measurements of total column ozone, total precipitable water wapor, aerosol optical depth (AOD) and the degree of cloud cover from the Moderate Resolution Imaging Spectroradiometer (MODIS) [13], the measurements of the total columns and vertical profiles of ozone, water vapor (H_2O), carbon monoxide (CO) and methane (CH_4) from the Advanced Infrared Sounder (AIRS) [14], and total column CO measurements from the MOPITT (Measurements Of Pollution In The Troposphere) instrument [15]. Ozone measurements at the stations of the world ozonometric network from the WOUDC archive, upper-air measurements at the stations of the world aerological network from the archive of the University of Wyoming, NCEP/NCAR reanalysis data [16] and active fires, detected by the MODIS instruments [17] were also involved in the analysis. Data used in this work as well as their sources are collected in table 1. It can be seen from the table 1 that a significant part of data was obtained from the NASA / Giovanni server [18].

Table 1. Data used in this work and their sources

Data (spatial resolution)	Web address
OMI (UV, O_3: 1° × 1°, CH_2O, NO_2: 0.25° × 0.25°)	http://disc.sci.gsfc.nasa.gov/giovanni
MLS (400-500 км)	http://disc.sci.gsfc.nasa.gov/giovanni
MODIS (1° × 1°)	http://disc.sci.gsfc.nasa.gov/giovanni http://ladsweb.nascom.nasa.gov
AIRS (1° × 1°)	http://disc.sci.gsfc.nasa.gov/giovanni
MOPITT (1° × 1°)	http://eosweb.larc.nasa.gov
WOUDC	https://woudc.org
Upper-air data	http://www.weather.uwyo.edu/upperair
Active fires: MODIS /Terra (1 км × 1 км)	https://earthdata.nasa.gov/earth-observation-data/near-real-time/firms

3. Methods

To extract the effects of atmospheric blocking events, against the background of significant natural atmospheric variability, along with the analysis of measured characteristics, the anomalies of atmospheric parameters (Δ) were also analyzed. Spatial (longitude-latitude) distributions of anomalies were characterized by deviations of local values of atmospheric parameters averaged over blocking periods from the corresponding local long-term means. Temporal variations of regional mean anomalies were characterized by deviations of current everyday regional mean values of atmospheric parameters from the long-term regional mean values corresponding to a given day.

4. Results and discussion

4.1. Changes in the atmospheric composition associated with pyrogenic emission

Prolonged summer atmospheric blocks are accompanied by the heat waves, lack of precipitation and soil drought, which is favorable for the development of wildfires. In the summer of 2012, an unusually hot weather in Siberia was caused by a series of blocking anticyclones conducive for frequent influxes in the region of hot and dry air from Central Asia. Extreme weather regime led to the development of massive forest fires (figure 1a). Figures 1b-1e show daily variations of the total number of active fires in European Russia (ER): 50°-70°N, 20°-60°E), Western Siberia (WS): 50°-70°N, 60°-100°E), Eastern Siberia (ES): 50°-70°N, 100°-140°E) and Far East (FE): 50°-70°N, 140°-180°E) during the summer of 2012 according to the active fire detection data from the MODIS/Terra instrument. In the same figures, the daily variations in the regional mean aerosol optical depth (AOD) calculated using MODIS

data and the variations of total column CO calculated using MOPITT data are also presented (AOT during massive wildfires is determined mainly by the concentration of the smoke particles in the air).

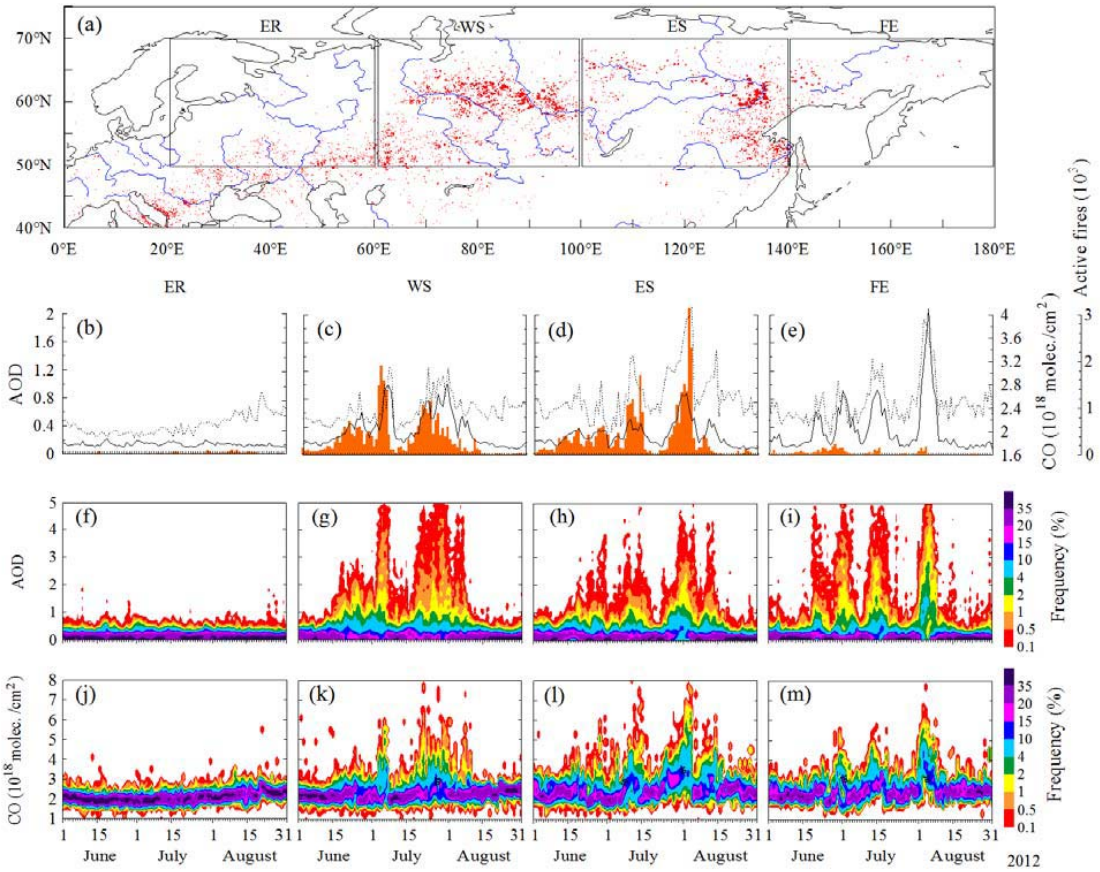

Figure 1. Spatial distribution of active fires over Northern Eurasia in the summer of 2012 (a), daily variations of active fires (color filling), AOD at the wavelength 550 nm (solid curve) and the total column of CO (dashed curve) in/over ER (b), WS (c), ES (d) and FE (e), everyday EPDs of AOD over ER (f), WS (g), ES (h) and FE (i) and everyday EPDs of total column CO over ER (j), WS (k), ES (l) and FE (m) in June-August 2012.

The regional mean AOD values over ER in the summer of 2012 were close to the background (0.13). The increase in the content of CO in the atmosphere in August was due to the seasonal course of total column CO [19]. With a small number of relatively weak fires, mainly in the steppe zone, ER was characterized by a lack of correlation between the variations in the total number of fires and the regional mean values of AOT and CO (figure 1b) and also by weak correlation of the AOT and CO variations between themselves (r = -0.3). The latter is explained by the fact that, in the absence of massive wildfires, the sources of aerosol and CO in the atmosphere are, generally speaking, different.

The number of active fires in WS (ES) in the summer of 2012 was 20 (25) times as much that in ER (figure 1a). With the increase in fire activity, the regional mean AOT and CO over WS (ES) reached the values of 1.01 and $3.11 \cdot 10^{18}$ mollecules/cm^2 (0.88 and $4.15 \cdot 10^{18}$ molecules/cm^2), respectively. The regional mean AOT during wildfires increased 5-6 times relatively to a pre-fire period, while the regional mean total column of CO increased 1.5-1.8 times. There was a high correlation between the variations of the regional mean values of AOT and CO with the regional fire activity (fig-

ures 1c, d), and also there was a close relationship between the variations of regional AOT and CO between themselves (r = 0.7). It was because during massive forest fires both AOT and total column CO are determined, mainly, by pyrogenic emission of aerosol particles and CO molecules in the process of biomass combustion.

The number of active fires in FE in the summer of 2012 was small (figure 1a), at that the variations of the regional mean AOD and total column CO weakly correlated with the regional fire activity. Therefore the high regional mean values of AOD and CO (up to 2.08 and 3.92·1018 mollecules/cm^2) and a high correlation between the regional means AOD and CO (r = 0.8), typical for air masses contaminated with combustion products, seem rather unexpected (figure 1e). This feature can be associated with the long-range atmospheric transport of combustion products from the Eastern Siberia forest fires into FE. The analysis showed that the regional mean AOD and CO over FE in the summer of 2012 positively correlated with the mean zonal wind u over the region between ES and FE (55°-65°N, 120°-150°E). The maximum correlation between AOD and CO with u achieved with wind taken at the level of 300 hPa (0.61 and 0.50, respectively).

Long-range transport of combustion products is one of the modern global problems, since it can lead to strong pollution of the atmosphere of regions distanced at hundreds or even thousands kilometers from the forest fires. The cases of long-range atmospheric transport of combustion products from the Siberian forest fires to the east have been repeatedly noted [20]. These are due to the predominance of the western winds in the mid-latitude troposphere. The cases of anomalous transport of combustion products (from east to west) are more rare. The physical mechanisms responsible for the transport of smoke and CO from the forest fires in Siberia to Central Europe in July 2016 were investigated in [21, 22]. The results of the analysis showed that the eastern long-range transport in the atmosphere of the combustion products was favored by predominant location in the center of Eurasia of a high-pressure system (anticyclone) to the north of a low-pressure one (cyclone) characteristic for atmospheric blocking of the dipole type. Because in an anticyclone air circulates clockwise, while in a cyclone - counterclockwise, at the boundary of high- and low pressure systems (which was located near the 60N), air was transferred from east to west. It was shown that the anomalous transport of combustion products from Siberian forest fires occurred at a distance of about 5000 km with a speed of about 5 m/s. The case of anomalous transboundary long-range transfer of smoke from the North American forest fires into the territory of Russia in August 2004 was revealed in [23]. The latter event was also conditioned by the peculiarities of atmospheric circulation, which are characteristic for the atmospheric blocking of the dipole type, with the anticyclone over the Chukchi Sea and the cyclone over the south of the Barents Sea. In contrast with the western transport, which is the most intensive in the upper troposphere, the eastern transport of combustion products occurred mainly in the lower troposphere.

Using the mean values for representation of AOD and CO variations (figures 1b-d) during the periods of massive forest fires is not quite correct due to essential distinctions of the AOT and CO probability distributions functions from normal ones. More complete and adequate information about AOT and CO variation during wildfires gives an analysis of changes in the empirical probability distributions (EPDs) of AOD (figure 1f-1i) and CO (figure 1j-m) over the regions under consideration. According to MODIS data, over WS at the end of July and over FE in early August, AOD values at the wavelength of 550 nm and in spatial resolution 1 ° × 1 ° (L3) reached 5 that is 30-40 times the AOD values in the pre-fire period. This also means that part of AOD values at the original resolution of 10 km × 10 km (L2) exceeded 5 and indicates the need to extend the upper limit of the operating range of the MODIS algorithm. According to MOPITT data, the total column CO during the maximum development of forest fires in Siberia at a resolution of 1° × 1° reached $8 \cdot 10^{18}$ molecules/cm^2 that is 3-4 times the values of CO contents in the pre-fire period.

Over the areas of intense forest fires, accompanied summer atmospheric blocking events over ER in 2010 and WS in 2012, an increase in the atmospheric total column of CH_2O and tropospheric column of NO_2 was revealed [24]. Due to the short lifetime of CH_2O and NO_2 molecules in the atmosphere, the increase of formaldehyde and nitrogen dioxide in the atmosphere over foci of burning can be related to the pyrogenic emission of CH_2O and NO_2 when biomass combustion. Over the clusters of

the most intense fires in ER (52°-57°N, 38°-49°E) in the period of their maximum development (1-10 August 2010) and over those in WS (57°-62°N, 85°-98°E; 22-31 July 2012), the regional mean contents of CH_2O amounted to $2.45 \cdot 10^{16}$ molecules/cm^2 and $1.47 \cdot 10^{16}$ molecules/cm^2, respectively, that 2 times the content of CH_2O over these areas in the absence of wildfires.

The maximum daily total column of CH_2O over ER (WS) in the spatial resolution 0.25° × 0.25° reached $9.3 \cdot 10^{16}$ ($1.0 \cdot 10^{17}$) molecules/ cm^2, respectively. The mean tropospheric columns of NO_2 over the same areas and in the same periods achieved the values $2.0 \cdot 10^{15}$ ($1.2 \cdot 10^{15}$) molecules/cm^2, which is 1.2 times the corresponding NO_2 contents in the absence of fires. The daily local NO_2 content in the atmosphere over ER (WS) in the resolution 0.25° × 0.25° reached the values of $2.5 \cdot 10^{16}$ ($1.2 \cdot 10^{16}$) molecules/cm^2, respectively. The ratio of the regional total column of CH_2O to the regional tropospheric column of NO_2 over ER and WS was dependent on the regional fire activity. Over both the regions, in the absence of fires the ratio of CH_2O to NO_2 was 7-8, while in periods of maximum fire development it increased up to 12.

4.2. *Changes in the atmospheric composition associated with biogenic emission*

An increase in the content of CH_2O revealed itself not only over the foci of burning but also in the atmosphere over ER and WS in the whole. According to OMI data, the daily regional mean CH_2O content over ER in the summer of 2010 and over the WS in the summer of 2012 reached $1.7 \cdot 10^{16}$ molecules/cm^2 and $1.4 \cdot 10^{16}$ molecules/cm^2, respectively (an increase of 72% and 55% relatively to the corresponding long-term values of the CH_2O contents). As an example, figures 2 show the changes in the CH_2O content over the region restricted by coordinates 45°-65°N, 30°-60°E in May-September 2010. Significant differences in the EPDs of CH_2O during the periods of high and low fire activity were revealed (figure 2b). It can be seen that the modal values of CH_2O during pre-fire period and during wildfires 2010 were $8.5 \cdot 10^{15}$ molecules/cm^2 and $14.5 \cdot 10^{15}$ molecules/cm^2, respectively. The EPD of CH_2O during wildfires was characterized by 1.5 times a half-width than EPD in the absence of fires. These differences indicate the effect of pyrogenic emission of CH_2O on the regional content of formaldehyde. At the same time, the local maxima of short-lived CH_2O anomalies (the lifetime of the CH_2O molecule in the troposphere are several hours) are generally weakly related to the spatial distribution of active fires (figure 2a). It can be seen that the vast region of increased CH_2O content rather coincides with the region of surface temperature anomalies exceeding 10°C and agrees with the wind field in the lower troposphere.

The results of the analysis indicate a close connection between the daily regional mean CH_2O anomalies over ER and WS (ΔCH_2O) with regional surface temperature anomalies (ΔT_s), which is characteristic for both the fire periods and the quiet periods [24]. Over ER, a high positive correlation between regional mean anomalies of ΔCH_2O and ΔT_s ($r = 0.81$) was revealed, in particular, in the pre-fire period: 1 May - 22 July 22 (figure 2c). The connection between ΔCH_2O and ΔT_s in this period is close to linear. Based on linear regression, the sensitivity of the daily regional mean total column CH_2O anomaly to the corresponding anomaly of T_s in the pre-fire period was estimated as $\Delta CH_2O/\Delta Ts = 0.45 \cdot 10^{15}$ molecules·cm^{-2}/°C or 4.5%/°C (relatively to corresponding long-term CH_2O content). During the period of massive wildfires in ER (from 23 July till 16 August) the dependence of ΔCH_2O on ΔT_s was nonlinear and can be closer approximated by the exponential function $\Delta CH_2O = 2.05 \exp(0.165 \cdot \Delta T_s)$, where ΔCH_2O is expressed in 10^{15} molecules/cm^2, ΔT_s is in °C (coefficient of determination (R^2) of exponential (linear) approximation is 0.85 (0.74), respectively).

A positive correlation of total column CH_2O content in the atmosphere with a surface temperature is probably due to the photochemical formation of formaldehyde in the atmosphere due to oxidation of isoprene (C_5H_8) emitted by plants. In unfavorable for plant conditions associated with summer atmospheric blocking events (anomalous increase of surface temperature, prolonged sun shining and soil drought), the biogenic emission of isoprene increases, reaching a maximum at 35-40°C [3].

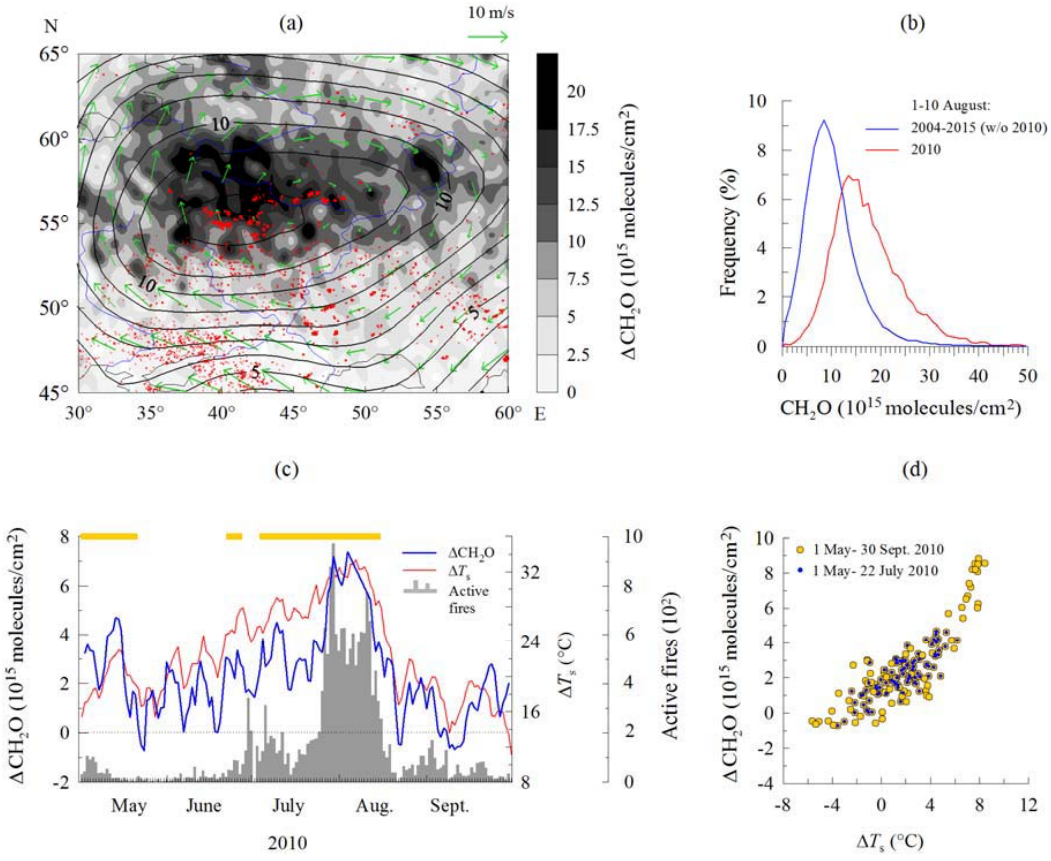

Figure 2. (a) Spatial distributions of ΔCH_2O (tonal gradation), active fires (small red crosses), temperature anomalies at the pressure level of 1000 hPa (isolines, labels in °C) and the vectors of 850-hPa wind (green arrows) during 1-10 August 2010, (b) the EPDs of CH_2O over the region (45°-65°N, 30°-60°E, hereafter also ER) under atmospheric blocking and without it, (c) daily regional mean anomalies of CH_2O and *T*s over ER as well as daily total number of active fires in the same region in May-September 2010 (horizontal orange bars denote the episodes of atmospheric blocking over ER), (d) scatter plot between daily regional mean ΔCH_2O values over ER versus corresponding ΔT_s values in May – September 2010 (yellow circles) and that during the pre-fire period in ER in 2010 (blue circles).

4.3. *Changes in the atmospheric composition associated with soil emission*

In the summer of 2016 the north of WS was characterized by anomalously hot weather, whose reason was a prolonged location an extensive high-pressure region in the subarctic zone, to the south of which a low-pressure region was located. As already noted, such disposition of the pressure systems is typical for the dipole type of atmospheric blocking (figure 3a). In the high pressure region, the strong positive anomalies of surface temperature occurred with maximum values of ΔT_s up to 10°C in the Yamal Peninsula (figure 3a).

Analysis of AIRS data showed that the spatial distribution of the anomalies of CH4 over the north of the WS, both total column (TC) and volume mixing ratio (VMR) of CH_4 in the free troposphere, were also characterized by positive values (figure 3c) with local (1° × 1°) total column CH_4 maxima

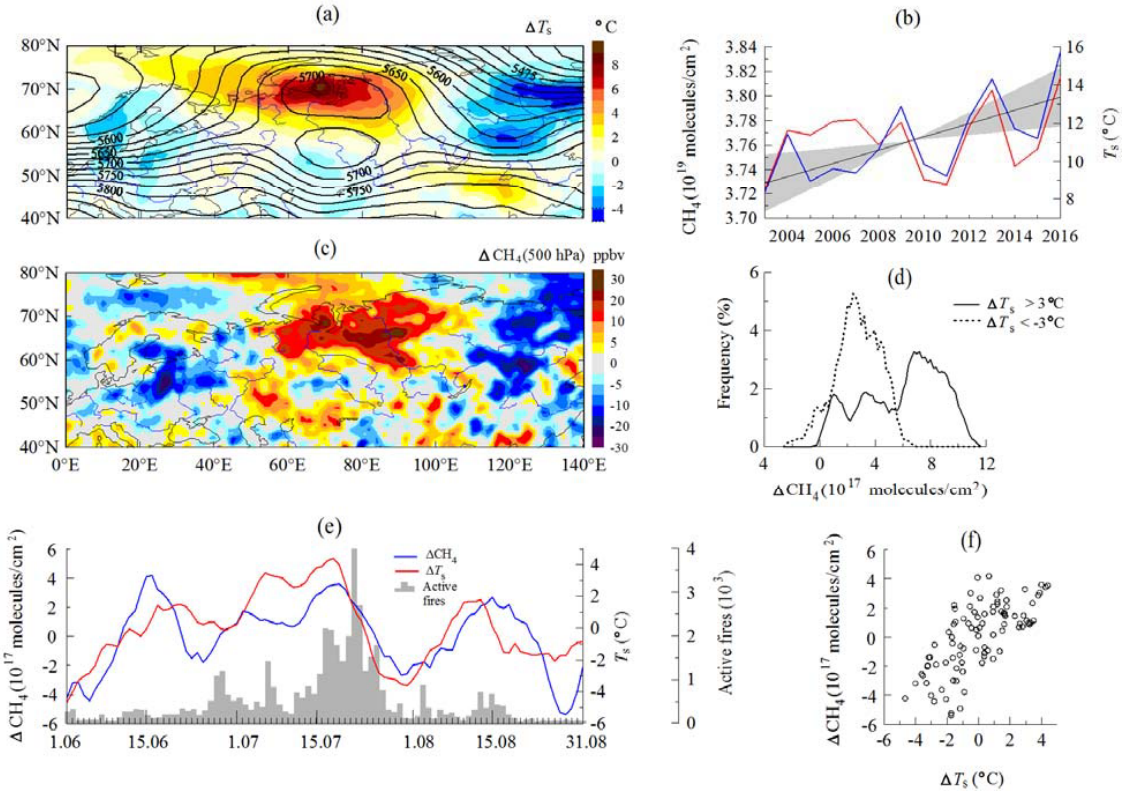

Figure 3. (a) 500-hPa geopotential height field (isolines, labels in geopotential meters) and surface temperature anomalies (ΔT_s, color scale) during 1-20 July 2016, (b) regional mean total column methane content and regional mean surface temperature over the north of Western Siberia (WS: 65°-75°N, 60°-100°E) in July in the period of 2003-2016; the linear trend of CH_4 (straight line) and its 95% confidence intervals (shading) are also shown, (c) anomalies of the methane volume mixing ratio (ΔCH_4) at the pressure level of 500 hPa during 1-20 July 2016, (d) the EPDs of ΔCH_4 over the territory of Northern Eurasia (50°-80°N, 0°-140°E) at ΔT_s less than -3°C and at ΔT_s more than 3°C, (e) the everyday regional mean values of ΔCH_4 and ΔT_s over the north of WS and the number of active fires in Siberia (55°-75°N, 60°-120°E), (f) scatter plot of the everyday regional mean values of ΔCH_4 versus ΔT_s over the north of WS in the summer of 2016.

over Yamal ($5.7 \cdot 10^{17}$ molecules/cm^2 or 1.5% relatively to corresponding long-term value of TC CH_4 in Julies 2003-2015), Taimyr ($6.2 \cdot 10^{17}$ molecules/cm^2 or 1.6%) and near Igarka ($6.5 \cdot 10^{17}$ molecules/cm^2 molecules/cm^2 or 1.8%) and with local maxima of CH_4 VMR (at 500-hPa level) over Yamal (27 ppbv or 1.5%) and Putorana Plateau (30 ppbv or 1.6%). The positive anomalies of methane, detected over the north of WS in the summer of 2016, were comparable with the intra-annual variations of CH_4 over this region.

Comparison of figure 3c with figure 3a indicates the similarity of the spatial distributions of ΔCH_4 and ΔT_s with the longitude alternation of regions with different signs of the anomalies in the subpolar and polar latitudes. It is known that the changes in land surface temperature, along with changes in soil moisture and water table depth, regulate the soil emission of carbon-containing compounds [25]. In the cryolitizone, in particular, an increase in surface temperature leads to thawing of the permafrost and contributes to an increase in methane emissions from wetlands [5].

The relationship between the spatial distributions of ΔT_s and ΔCH_4 also manifests itself in the principal distinction of the EPDs of ΔCH_4 under different temperature regimes (figure 3d). It can be seen

from that at $\Delta T_s < -3$°C, the EPD of ΔCH_4 is unimodal with a peak at about $2 \cdot 10^{17}$ molecules/cm^2, whereas at $\Delta T_s > 3$°C the distribution of ΔCH_4 is polymodal, with the main peak centered at $7 \cdot 10^{17}$ molecules/cm^2, which is accompanying by two additional minor peaks at $1 \cdot 10^{17}$ molecules/cm^2 and at $3 \cdot 10^{17}$ molecules/cm^2.

Correlation between variations of the daily regional mean anomalies of CH_4 and T_s was also revealed (figure 3e). It can be seen that each of heat waves occurred in the north of WS in the summer of 2016 was accompanied by an increase in the regional abundance of CH_4. The results of the analysis show that on the formation of positive correlation of ΔCH_4 and ΔT_s the intra-seasonal variations of CH_4 and T_s (with the period exceeding the characteristic synoptic period) contributed significantly. This inference is confirmed by the results of cross-wavelet analysis of ΔCH_4 with ΔT_s - their statistically significant coherence manifests itself for the periods of about 3 weeks or more. When using linear regression (figure 3f), the sensitivity of daily anomalies of the regional total column of CH_4 to the corresponding anomalies of surface temperature was estimated to be $\Delta CH_4/\Delta T_s = 7.5 \cdot 10^{16}$ molecules·cm^{-2}/°C or 0.2% /°C, relatively the average regional mean total column of CH_4 in Julies of 2003-2007 ($3.74 \cdot 10^{19}$ molecules/cm^2) [26].

It is known that the wildfires are an important natural source of methane in the atmosphere. In the summer of 2016, massive fires in Siberia were concentrated to the south of the region of the increased atmospheric CH_4 content. Atmospheric circulation promoted the transport of combustion products south of the region characterized by the positive anomaly of CH_4 in the atmosphere - approximately along 60°N [21, 22]. A conducted correlation analysis did not reveal any significant correlation between the variations of CH_4 over the north of WS with forest fire activity in the territory of Siberia (figure 4e).

Over the north of WS the connection between methane content in the regional atmosphere and surface temperature is also manifested in the interannual variations of CH_4 and T_s (figure 3b). The regional mean July values of CH_4 and T_s in 2003-2016 as a whole positively correlate with each other (the only failure occurred in 2006-2008). The positive correlation between the July values of CH_4 and T_s is partly related to the unidirectional trends of CH_4 and T_s observed in this region during the period of 2003-2016. Changes in July's methane contents over the north of WS in this period were characterized by a positive linear trend of 5.4 ($\pm$ 3.6)$\cdot 10^{16}$ molecules·cm^{-2}/year or 1.5 ($\pm$1.0)%/10 years, statistically significant at 0.05 level (in parentheses - $\pm$ 95% confidence intervals for the trend). The corresponding changes in the surface temperature were also characterized by a positive linear trend 1.1 ($\pm$ 2.5) °C/10 years, which was however statistically insignificant. After removal of linear trends and using linear regression, the sensitivity of the interannual variations of the regional mean CH_4 content to variations of regional mean T_s was estimated to be $CH_4/T_s = 1.1 \cdot 10^{17}$ molecules·cm^{-2}/°C or 0.3%/° C [26]. It is characteristic that the sensitivity of CH_4 to T_s at the interannual time scale is higher than that at the synoptic scale.

4.4. *Changes in the atmospheric composition associated with atmospheric dynamics*

An analysis of satellite, aerological and ozonesonde data indicate an increase in water vapor (WV) and decrease of ozone contents over the regions of atmospheric blocking [27-29]. According to AIRS data, total column water vapor (TCWV) in the area of the blocking anticyclone over ER in the summer of 2010 was characterized by positive anomalies, reaching the values of 11 kg/m^2 (or 54% relatively corresponding long-term mean values) (figure 4c), while total column ozone (TCO) was characterized by negative anomalies with the local values down to -33 Dobson units (DU) or -10% (figure 4d). At the same time the regions adjacent to the blocking area to the east and west, on the contrary, were characterized by positive anomalies of TCO (up to 50 DU) and by negative anomalies of TCWV (-4 kg/m^2). During the summer atmospheric blocking event over ER in 2010, the statistically significant negative spatial correlation between the anomalies of TCO and TCWV over the northwest of Eurasia (45°-75°N, 15°W-105°E) was revealed: $r = -0.71$ (with 95% confidence interval -0.73, -0.69) [9].

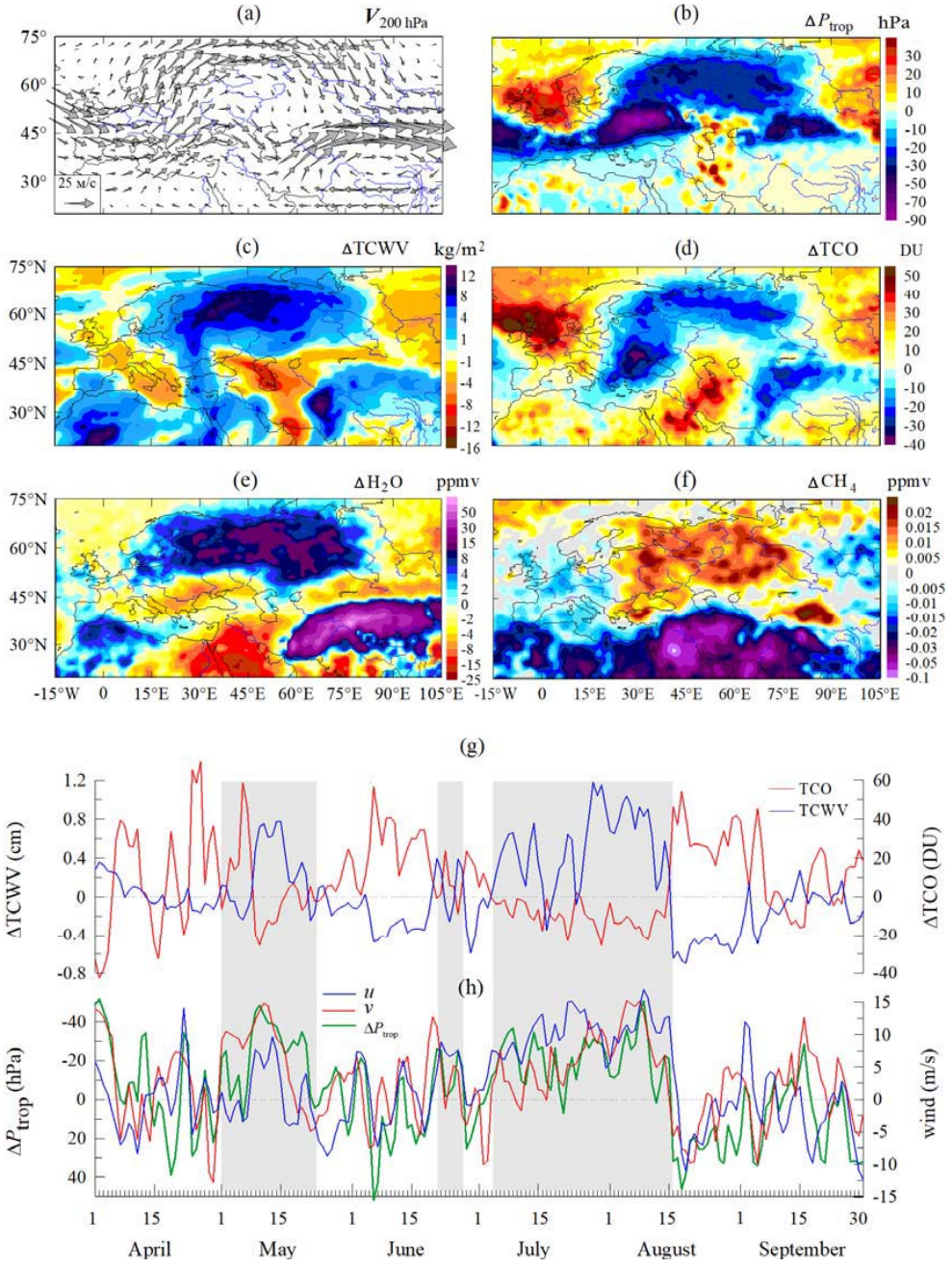

Figure 4. Spatial distributions of: (a) 200-hPa wind (V_{200}), (b) tropopause pressure anomalies (ΔP_{trop}), (c) total column water vapor anomalies (ΔTCWV), (d) total column ozone anomalies (ΔTCO), (e) 200-hPa water vapor mixing ratio anomalies (ΔH_2O), (f) 160.5-hPa methane mixing ratio anomalies (ΔCH_4) averaged over the period 1-10 August 2010; temporal variations of the regional mean values of: (g) ΔTCO and ΔTCWV over the region (60°-70°N, 30°-60°E), (h) ΔP_{trop} averaged over the same region as well as the meridional wind (v) averaged over the Central European region (45°-75°N, 15°-30°E) and zonal wind (u) averaged over the polar region (65°-75°N, 30°-60°E) (the data are from the AIRS instrument, excepting wind data, which are taken from the NCEP/NCAR reanalysis, shading denotes atmospheric blocking episodes).

The increase in TCWV and decrease in TCO over the blocks were mainly due to dynamic causes and related to the peculiarities of regional atmospheric circulation during omega-blocking, namely by the quasi-horizontal advection of the enriched by water vapor but ozone depleted subtropical air to the north of ER above the western and northern periphery of the blocking anticyclones (figure 4a) as well as by the increase in tropopause height (cf. figures 4c and 4d with figures 4a and 4b). In addition, the decrease in TCO can be partially attributed to the photochemical destruction of ozone due to the advection of WV through the tropopause gap directly from the low-latitude troposphere to the lower stratosphere above the block and thus intensification the processes of ozone depletion in the hydrogen catalytic cycle in the lower stratosphere [30].

Using linear regression model, the sensitivity of regional TCO and TCWV anomalies over the north of ER (60°-70°N, 30°-60°E) to changes in the position of regional tropopause during the summer of 2010 was estimated to be $\Delta TCO/\Delta P_{trop}$ = 0.90 DU/hPa and $\Delta TCVW/\Delta P_{trop}$ = -0.86 cm/hPa (where P_{trop} is pressure at the tropopause level). The relation between TCO and TCWV within blocked area with variations of the zonal wind u above the northern periphery of anticyclone (65°-75°N, 30°-60°E) and with the meridional wind v above the western periphery of anticyclone (45°-75°N, 15°-30°E) was also investigated. The variations of u and v over the selected regions give an idea of the intensity of the anticyclonic circulation over ER during atmospheric blocking events. The closest coupling between the TCO and TCWV anomalies within the block with u and v revealed itself with the wind components taken at the pressure level of 200 hPa. In the mid-latitudes this level is close to the tropopause region that indicates the key role of the wave - vortex dynamics in the formation of the regional TCO and TCWV anomalies during omega-blocking events over ER. The sensitivities of regional mean ΔTCO and ΔTCWV over the north of ER to the variations of u and v at the 200-hPa level were estimated to be: $\Delta TCO/u$ = -0.87 DU/m·s^{-1}, $\Delta TCWV/u$ = 0.78 cm/m·s^{-1}, $\Delta TCO/v$ = -0.65 DU/m·s^{-1}, $\Delta TCWV/v$ = 0.69 cm/m·s^{-1}.

The positive anomalies of CH_4 (up to 20 ppb) was found in the lower stratosphere over ER during the summer 2010 atmospheric blocking event (figure 4f). Since the climatological distribution of methane in the stratosphere is characterized by a decrease from south to north, the increase in CH_4 in the lower stratosphere over the blocked region could also be due to the advection of the methane enriched air from low latitudes to the north of ER in the rear part of stratospheric anticyclone, which accompanied the blocking anticyclone in the troposphere [8, 9].

The vertical structure of the ozone anomalies within blocking area during the spring and summer atmospheric blocking events over ER in 2010 was characterized by negative anomalies in the troposphere and lower stratosphere and by the dominance of the positive O_3 anomalies in the middle and upper stratosphere. The negative anomalies of ozone reached -0.18 ppmv at 150 hPa (-23% relatively the long-term volume mixing ratio of ozone at the specified level) during the spring event and -0.26 ppm (-11%) at 50 hPa during the summer one. The corresponding WV profiles were characterized by the positive anomalies of H_2O in the troposphere and lower stratosphere, reaching the values of 3.5 × 10^{-3} in the lower troposphere and 3.2 ppm (39%) in the lower stratosphere during the spring block and the values of 6 × 10^{-3} in the lower troposphere and 6.6 ppm (43%) in the lower stratosphere during the summer block [9, 29].

Because TCO modulates the intensity of solar UV radiation incoming to the Earth's surface, the decrease in TCO during atmospheric blocking events, cloudless anticyclonic weather and the high position of the Sun in the summer can result the living things within the blocking areas will be exposed by hazardous doses of biologically active solar radiation [31]. Based on the measurements of TCO and UV radiation from the OMI instrument, an analysis was made of the spatial and temporal variations of the solar UV exposure during atmospheric blocks over ER in the spring and summer 2010.

The results indicated a significant increase of the surface biologically active solar UV radiation in the blocking areas. During the summer atmospheric block (figure 5a), the maximum erythemal UV daily doses (ΔUV) were observed over Southern Ural (534 J/m^2 or 17% relative to the corresponding long-term mean), Western Caucasus (1040 J/m^2 or 21%) and the north-east of ER (631 J/m^2 or 23%) (figure 5a). There is a close conformity between the spatial distributions of ΔUV and ΔTCO during the

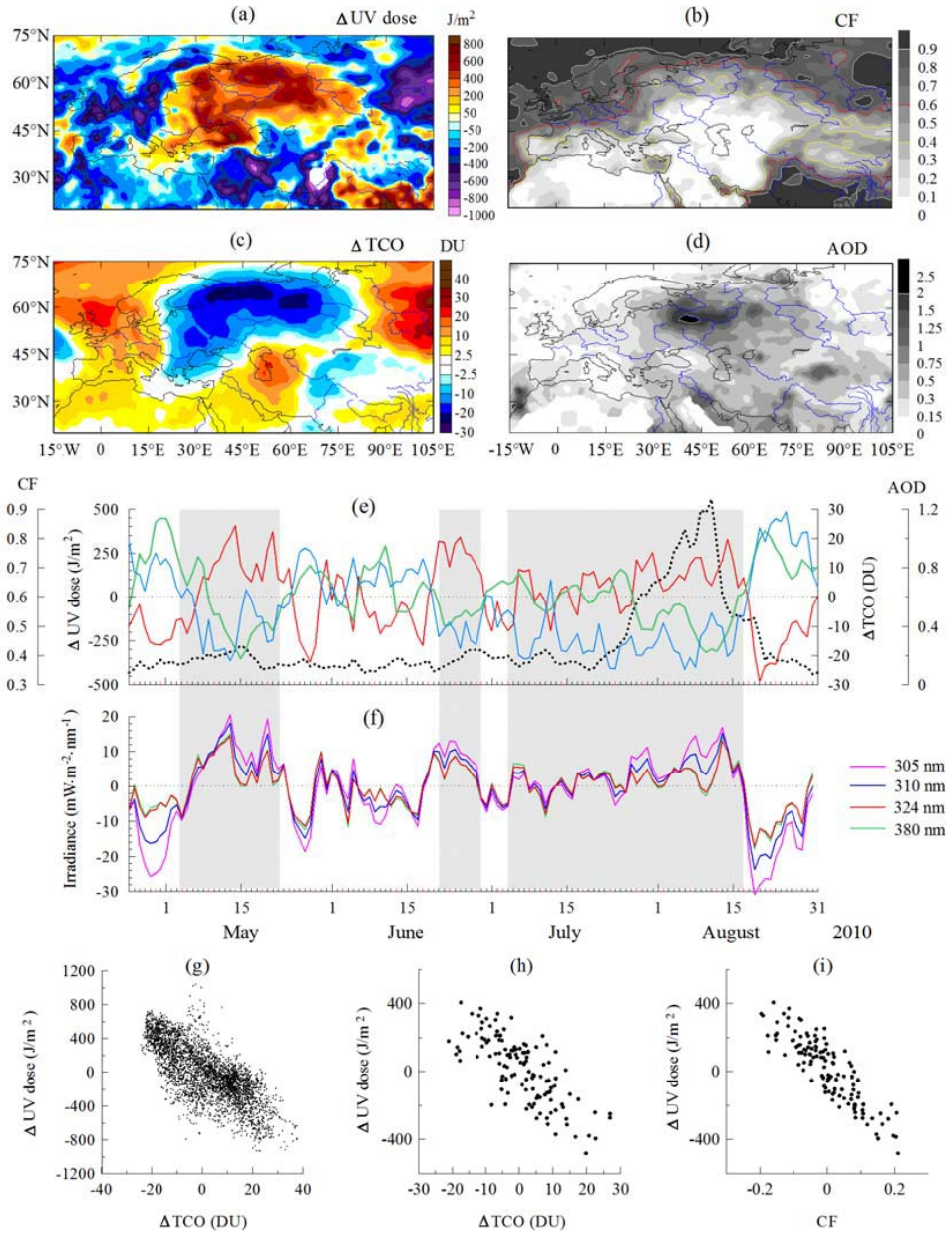

Figure 5. Spatial distributions over the period 1-10 August 2010 of: (a) the anomalies of erythemal UV daily dose (ΔUV dose), (b) CF, (c) ΔTCO and (d) AOD (λ=550 nm); the time series of: (e) the daily regional mean ΔUV dose and ΔTCO as well as daily regional CF and AOD over the region (50°-70°N, 30°-70°E), (f) daily regional mean surface UV irradiances over the same region in the summer of 2010; the scatter plots of: (g) the mean local (1° × 1°) ΔUV dose in the region (40°-75°N, 15°W-105°E) 1-10 August 2010 versus corresponding local ΔTCO, (h) the daily regional mean ΔUV dose UV over (50°-70°N, 30°-70°E) versus corresponding anomalies of the daily regional mean ΔTCO and (i) the daily regional mean ΔUV dose UV over (50°-70°N, 30°-70°E) versus the daily regional mean CF. The time-series of ΔUV, ΔTCO and surface irradiances as well as CF in (i) were filtered by subtraction from daily data the corresponding 31-day running mean values; shading denotes blocking episodes.

blocking period: in the middle and high latitudes, both the ΔUV and ΔTCO distributions revealed the alternation in signs with longitude and both of them manifest the similar wave-vortex structures associated with the regional features of the large-scale atmospheric circulation during omega blocks over ER (cf. figure 5a with figure 5c). There is a high spatial anticorrelation between the local (1° × 1°) ΔUV and ΔTCO for the region restricted by the coordinates 40° -70°N, 15°W-105°E (r = -0.75). The sensitivity of the local UV anomalies in the abovementioned region averaged over the period 1-10 August 2010 to corresponding TCO anomalies was obtained to be: ΔUV/ΔTCO = -19 J m^{-2}/DU (figure 5g). In May-August 2010 a high anticorrelation between the regional mean everyday ΔUV alues and ΔTCO values was also observed (r = -0.74) with the regular decrease in ΔTCO and increase in ΔUV in the periods of atmospheric blocking (figure 5d). An increase in irradiances at individual wavelengths in the UV region during atmospheric blocking events was also observed with the greatest change of irradiance at the wavelength of 305 nm, where the ozone absorption of the solar UV radiation is very strong (figure 5f). The sensitivity of the regional mean ΔUV to corresponding ΔTCO was estimated to be ΔUV/ΔTCO = -14 J m^{-2}/DU (figure 5h). The presented results show that the increase of the erythemal UV dose in the periods of atmospheric blocking over ER in the spring and summer of 2010 at least in part was due to a decrease in TCO, observed during blocks over the given region.

Alongside with TCO, cloudiness has strong effect on the surface UV radiation. Using MODIS cloud product, the relation between UV radiation and cloud fraction (CF) during the atmospheric blockings over ER in spring and summer 2010 was analyzed. The spatial distributions of CF during the blocking periods evidence the cloudless weather regime in the south and center of ER (figure 5b) with the more denser cloud cover over the western, northern and eastern peripheries of the blocking anticyclones (CF = 0.7-0.9). During the summer block, the shape and position of the isohypse CF = 0.7 north of 50°N approximately coincided with the boundary between the positive and negative UV anomalies (cf. figure 5a and figure 5b). The correlation analysis of the daily regional means of ΔUV and CF indicates a close correlation between the anomalies in UV and ΔCF at synoptic time scales, at that the correlation between ΔUV and CF variations was higher than that that between ΔUV and ΔTCO (-0.87 and -0.74, respectively). Thus the increase in surface UV radiation during atmospheric blocking events over ER in spring and summer 2010 was also related to the decrease of cloud cover over the region occupied by the blocking anticyclones.

An important factors affecting surface UV radiation are the content of aerosol particles in the atmospheric column and the physical and microphysical characteristics of aerosols. Anomalously prolonged summer block over ER in 2010 was accompanied by the development of massive wildfires in the period from July 23 to August 16 that resulted in intensive pyrogenic emission of aerosol (smoke) particles into the atmosphere [32]. Analysis of the aerosol optical depth (AOD) measurements from the MODIS/Terra instrument showed that the average value of AOT at the wavelength λ = 550 nm exceeded 2 between Moscow and Kazan, with a local (1° × 1°) maximum of 2.54 over the east of the Vladimir region (56°-57°N, 41°-42°E) (figure 5d). In contrast with the spatial distributions of ΔUV and ΔTCO, characterized by extreme values over the western and northern peripheries of the block (figure 5a and 5c), the maximum AOD was localized in the center of the blocking anticyclone. A comparison of the spatial distributions of ΔUV (figure 5a) and AOT (figure 5d) shows that the region characterized by AOT > 2 coincides well with the region of minimum values of ΔUV at the center of ER (ΔUV dose < 300 J/m^2).

The decrease in surface UV radiation during the massive wildfires in ER was noted previously. According to the ground-based AOT measurements at AERONET Moscow _MSU_MO station, the local AOT values (λ = 500 nm) exceeded 6 on 7 August 2010, with local losses of erythemal UV radiation of 97% [33]. It should be noted, however, that the AOT field in this day was characterized by a strong spatial heterogeneity. The difference between AOT over the stations AERONET Moscow_MSU_MO and Zvenigorod (located 47 km west of Moscow) on 7 August 2010 reached 4. Figure 5e also shows temporal variations of the daily regional mean AOT over the region (50°-70°N, 30°-70° E) in the summer of 2010 according to MODIS/Terra data. The presented results indicate a sharp increase in AOT over this region in the period from 26 July to 11 August 2010 with a maximum of (1.27) on 11

August 2010. Characteristically, that with comparable cloud cover and similar reduction in CF during the spring and summer atmospheric blocks over ER in 2010, the surface UV irradiance during the summer block was lower than that during the spring one, that can be attributed to a strong smoke blanketing.

The conducted analysis revealed the main factors of changes in UV during the atmospheric blocking events over ER in spring and summer 2010. The results indicate that the decrease in TCO and decrease in cloud cover promoted the increase of UV over the periphery of blocking area, while the dense smoke in the center of ER, on the contrary, contributed to a reduction of UV. Since the presence of absorbing aerosols (smoke) in the lower troposphere leads to significant errors in the determination of surface UV radiation by the OMI instrument [34], the relative contribution of the above factors requires more in-depth analysis.

5. Conclusions

The analysis of data from satellite, balloon and ground-based systems for monitoring atmospheric contents of radiative and chemically active gas admixtures (O_3, H_2O, CO, NO_2, CH_2O, CH_4), as well as optical and microphysical characteristics of aerosol, revealed a number of key factors responsible for changes in the atmospheric composition under weather extremes and climatic anomalies associated with atmospheric blocking events in the regions of Northern Eurasia. The results of the analysis showed that most significant changes in the atmospheric composition were associated with the pyrogenic emission: under massive forest fires, often accompanying prolonged atmospheric blocks, AOT increases by 30-40 times, while the total column of CO - by 3-4 times. Along with the strong increase in AOT and CO, an increase in the local contents of CH_2O (by a factor of 2) and NO_2 (by a factor of 1.2) is observed over the clusters of intensive wildfires. The strong increase of surface temperature, prolonged sun shining and soil drought associated with summer atmospheric blocking events cause abiotic stress of vegetation in the blocking area. Under adverse conditions, as a protective reaction, plants increase emission of isoprene, the oxidation of which in the atmosphere leads to an increase in the regional abundance of CH_2O (70%). Under atmospheric blocking conditions in the subarctic zone, an increase in land surface temperature promotes the thawing of permafrost that increases the soil emission of CH_4 and thus the abundance of CH4 in the atmosphere over the blocking area (up to 2%). Along with the pyrogenic, biogenic and soil emissions, the causes of changes in the atmospheric composition during atmospheric blocking events are also regional features of large-scale atmospheric circulation. Due to advection of ozone depleted but water vapor enriched subtropical air accompanied by rising of the tropopause, a decrease in TCO (by 10-15%) and an increase in TCWV (by 50-70%) are noted in the blocking area. The decrease in TCO over the blocking area, cloudless weather and a high position of the Sun in the sky in summer, result in significant increase (up to 20%) of biologically active solar UV radiation coming to the Earth's surface. Under the atmospheric blocking of the dipole type, the peculiarities of atmospheric circulation promote to the long-range anomalous transfer of combustion products from east to west and can cause significant changes in the atmospheric composition over regions remote at a distance of thousands of kilometers from the region of wildfires.

Acknowlegements

This study was supported by the Russian Ministry of Education and Science, agreement № 14.616.21.0082 (RFMEFI61617X0082) with the use of results obtained in the RAS programs and RFBR projects.

References

[1] Obukhov A M, Kurgansky M V and Tatarskaya M C 1984 Dynamic conditions for the origin of drought and other large-scale weather anomalies (in Russian) *Meteorol. Hydrol.* **10** 5-13

[2] Andreae M O and Merlet P 2001 Emission of trace gases and aerosols from biomass burning *Glob. Biogeochem. Cycles.* **15** 955

[3] Guenther A B, Zimmerman P R, Harley P C, Monson R K and Fall R 1993 Isoprene and monoterpene emission rate variability: Model evaluations and sensitivity analyses *J. Geophys. Res.* **98** 12609
[4] Dufour G, Szopa S, Barkley M P, Boone C D, Perrin A, Palmer P I, Bernath P F et al 2010 Global upper-tropospheric formaldehyde: seasonal cycles observed by the ACE-FTS satellite instrument *Atmos. Chem. Phys.* **9** 3893
[5] Mokhov I I, Eliseev A V and Denisov S N 2007 Model diagnostics of variations in methane emissions by wetlands in the second half of the 20th century based on reanalysis data *Dokl. Earth Sci.* **417** 1293
[6] Orsolini Y and Nikulin G 2006 A low-ozone episode during the European heatwave of August 2003 *Q. J. R. Meteorol. Soc.* **132** 667
[7] Barriopedro D, Antón M and García GA 2010 Atmospheric blocking signatures in total ozone and ozone miniholes *J. Climate* **23** 3967
[8] Sitnov S A and Mokhov I I 2016 Satellite-derived peculiarities of total ozone field under atmos pheric blocking conditions over the European part of Russia in summer 2010 *Russ. Meteorol. Hydrol.* **41** 28
[9] Sitnov S A, Mokhov I I and Lupo A R 2017 Ozone, water vapor, and temperature anomalies associated with atmospheric blocking events over Eastern Europe in spring - summer 2010 *Atmos. Environ.* **164** 180
[10] Mokhov I I, Timazhev A V and Lupo A R 2014 Changes in atmospheric blocking characteris tics within Euro-Atlantic region and Northern Hemisphere as a whole in the 21st century from model simulations using RCP anthropogenic scenarios *Global Planet. Change* **122** 265
[11] Levelt P F, van den Oord G H J, Dobber M R, Malkki A, Visser H, de Vries J, Stammes P, Lundell J O V and Saari H 2006 The Ozone Monitoring Instrument *IEEE Trans. Geosci. Remote Sens.* **44** 1093
[12] Waters J W, Froidevaux L, Harwood R S, Jarnot R F, Pickett H M, Read W G, Siegel P H, Cofield R E, Filipiak M J, Flower D.A. et al 2006 The Earth observing system Microwave Limb Sounder (EOS MLS) on the Aura satellite *IEEE Trans. Geosci. Remote Sens.* **44** 1075
[13] Salomonson V V, Barnes W L, Maymon P W, Montgomery H E and Ostrow H 1989 MODIS, advanced facility instrument for studies of the Earth as a system *IEEE T. Geosci. Remote Sens.* **27** 145
[14] Aumann H H, Chahine M T, Gautier C, Goldberg M D, Kalnay E, McMillin L M, Revercomb H, Rosenkranz P W, Smith W L et al 2003 AIRS/AMSU/HSB on the Aqua mission: Design, science objectives, data products, and processing systems *IEEE Trans. Geosci. Remote Sens.* **41** 253
[15] Drummond J R and Mand G S 1996 The measurements of pollution in the troposhere (MOPITT) instrument: Overall perfomance and calibration requirements *J. Atmos. Oceanic Tech.* **13** 314
[16] Kistler R, Collins W, Saha S, White G, Woollen J, Kalnay E, Chelliah M, Ebisuzaki W, Kanamitsu M, Kousky V et al 2001 The NCEP-NCAR 50-year reanalysis: Monthly means CD–ROM and documentation *Bull. Amer. Meteor. Soc.* **82** 247
[17] Giglio L, Schroeder W and Justice C O 2016 The collection 6 MODIS active fire detection al gorithm and fire products *Rem. Sens. Environ.* **178** 31
[18] Acker J C and Leptoukh G 2007 Online analysis enhances use of NASA Earth science data *Eos Trans. AGU* **88** 14
[19] Sitnov S A, Mokhov I I and Dzhola A V 2017 Total content of carbon monoxide in the atmos phere over Russian regions according to satellite data *Izv. Atmos. Ocean. Phys.* **53** 32
[20] Teakles A, So R, Ainslie B, Nissen R, Schiller C, Vingarzan R, McKendry I, Macdonald A M, Jaffe D A, Bertram A K et al 2017 Impacts of the July 2012 Siberian fire plume on air quali ty in the Pacific Northwest *Atmos. Chem. Phys.* **17** 2593

[21] Sitnov S A, Mokhov I I and Gorchakov G I The link between smoke blanketing of European Russia in summer 2016, Siberian wildfires and anomalies of large-scale atmospheric circula tion *Dokl. Earth Sci.* **472** 190
[22] Sitnov S A, Mokhov I I, Gorchakov G I and Dzhola A V 2017 Smoke haze over the European part of Russia in the summer of 2016: A link to wildfires in Siberia and atmospheric circula tion anomalies *Russ. Meteorol. Hydrol*. **42** 518
[23] Sitnov S A and Mokhov I I 2017 Anomalous transboundary transport of the products of biomass burning from North American wildfires to Northern Eurasia *Dokl. Earth Sci.* **475** 832
[24] Sitnov S A and Mokhov I I 2017 Formaldehyde and nitrogen dioxide in the atmosphere during summer weather extremes and wildfires in European Russia in 2010 and Western Siberia in 2012 *Int. J. Remote Sens.* **38** 4086
[25] Smagin A V, Sadovnikova N B. Sherba T I and Shnyrev N A 2010 Abiotic factors of soil's res piration *The North Caucasus Ecological Herald* **6** 5
[26] Sitnov S A and Mokhov I I 2018 Anomalies in the atmospheric methane content over Northern Eurasia in the summer of 2016 *Dokl. Earth Sci.* **480** 637
[27] Sitnov S A and Mokhov I I 2013 Water vapor content in the atmosphere over European Russia during the summer 2010 fires *Izv. Atmos. Ocean. Phys.* **49** 414
[28] Sitnov S A, Mokhov I I and Lupo A R 2014 Evolution of water vapor plume over Eastern Eu rope during summer 2010 atmospheric blocking *Adv. Meteorol.* **2014** article ID 253953
[29] Sitnov S A and Mokhov I I 2015 Ozone mini-hole formation under prolonged blocking anticy clone conditions in the atmosphere over European Russia in summer 2010 *Dokl. Earth Sci.* **460** 41
[30] Anderson J G, Wilmouth D M, Smith J B and Sayres D S 2012 UV dosage levels in summer: Increased risk of ozone loss from convectively injected water vapor *Science* **337** 835
[31] Stick C, Kruger K, Schade N H, Sandmann H and Macke A 2006 Episode of unusual high solar ultraviolet radiation over central Europe due to dynamical reduced total ozone in May 2005 Atmos. Chem. Phys. 6 1771
[32] Sitnov S A, Gorchakov G I, Sviridenkov M A, Kopeikin V M, Ponomareva T Ya, and Karpov A V 2013 The effect of atmospheric circulation on the evolution and radiative forcing of smoke aerosol over European Russia during the summer of 2010 Izv. Atmos. Ocean. Phys. **49** 1006
[33] Chubarova N, Nezval' Ye, Sviridenkov M, Smirnov A and Slutsker I 2012 Smoke aerosol and its radiative effects during extreme fire event over Central Russia in summer 2010 Atmos. Meas. Tech. **5** 557
[34] McKenzie R L, Seckmeyer G, Bais A F, Kerr J B and Madronich S 2001 Satellite retrievals of erythemal UV dose compared with ground-based measurements at northern and southern midlatitudes J. Geophys. Res. **106** 24051